

UNIVERSITY OF CALIFORNIA - BERKELEY

UCRL-1542  
UNCLASSIFIED

cy 2.  
A

**TWO-WEEK LOAN COPY**

*This is a Library Circulating Copy  
which may be borrowed for two weeks.  
For a personal retention copy, call  
Tech. Info. Division, Ext. 5545*

**RADIATION LABORATORY**

## DISCLAIMER

This document was prepared as an account of work sponsored by the United States Government. While this document is believed to contain correct information, neither the United States Government nor any agency thereof, nor the Regents of the University of California, nor any of their employees, makes any warranty, express or implied, or assumes any legal responsibility for the accuracy, completeness, or usefulness of any information, apparatus, product, or process disclosed, or represents that its use would not infringe privately owned rights. Reference herein to any specific commercial product, process, or service by its trade name, trademark, manufacturer, or otherwise, does not necessarily constitute or imply its endorsement, recommendation, or favoring by the United States Government or any agency thereof, or the Regents of the University of California. The views and opinions of authors expressed herein do not necessarily state or reflect those of the United States Government or any agency thereof or the Regents of the University of California.

UCRL-1542

Unclassified-Physics Distribution

**UNCLASSIFIED**

UNIVERSITY OF CALIFORNIA

Radiation Laboratory

Contract No. W-7405-eng-48

FAST PROTONS FROM 270-MEV NEUTRON-DEUTERON COLLISIONS

James Warren Hadley

(Thesis)

November 5, 1951

Berkeley, California

TABLE OF CONTENTS

I Introduction

II General Experimental Procedure

III Details of Apparatus

A. Neutron Beam

B. Monitor

C. Magnetic Spectrometer

D. Counter Telescope

E. Scatterers

IV Reduction of Data

A. General Treatment of Data

B. Energy Intervals of Magnet Channels

C. Magnet Channel Efficiencies

D. Data Obtained with Magnet

E. Scattered Deuterons

F. Data Obtained with Counter Telescope

V Interpretation of Results

VI Acknowledgments

VII References

# FAST PROTONS FROM 270-MEV NEUTRON-DEUTERON COLLISIONS

James Warren Hadley

Radiation Laboratory, Department of Physics  
University of California, Berkeley, California

November 5, 1951

## I INTRODUCTION

Collisions of protons or neutrons with nuclei have generally been thought of in terms of interaction of the incident particle with the whole struck nucleus. According to this point of view, the incident particle may scatter elastically, without changing the internal energy of the nucleus from which it rebounds, or it may enter the nucleus and expend its energy in raising the nuclear temperature, resulting in the eventual expulsion of particles or photons in random directions. A transition region covering a rather wide energy interval occurs as bombarding energies are increased, however. Above energies of 100 Mev or so the wave length or effective size of the bombarding particle is no longer large with respect to separation distances of nucleons. As the energy of the incident particle increases through this region the particle tends more and more to interact with only one nucleon at a time, and the probability for its interaction with any nucleon decreases so that its mean free path within nuclear matter is large. The result of this transition is seen as a basic change in the nature of nucleon-nuclear collisions: with increasing energy, the collision products take on more and more the character of scattered particles from individual nucleon-nucleon collisions. The role of the struck nucleus passes from that of an integral and closely bound system to that of a cloud of separate scattering centers, each moving with a distribution in momentum

determined by its interaction with the rest of the nucleus, but otherwise free to act almost independently. One would expect that in the case of very high bombarding energies, emerging particles would be distributed in energy and angle almost as they are in the case of free nucleon-nucleon collisions. Illustrations of this state of affairs may be seen in recent reports on particles ejected from light elements by 240 and 340 Mev protons<sup>1,2</sup> and by 90 Mev neutrons<sup>3</sup>.

The special case of deuterium struck by high energy particles is of particular interest, because of the simplicity of the deuterium nucleus and the relative ease of theoretical treatment of its behavior in collisions. As suggested by the above remarks, one would expect the deuteron to behave very much as two separate particles when it is struck by neutrons of 200 to 300 Mev. It should be possible, in fact, to attribute various kinds of emergent particles to collisions of the incident neutron with either one or the other of the deuteron's components. The total scattering cross section can be expressed as a sum of the n-p cross section, the n-n cross section, and an additional term, probably small, resulting from interference of various kinds<sup>4,5,6</sup>.

Protons, in particular, resulting from n-d collisions, should fall roughly into two groups. A group at low energies would result partly from n-n collisions which carry away both neutrons, leaving the proton in about the same state of motion that it was in at the time of collision, and partly from n-p collisions in which no charge exchange takes place. The second group, at energies of the order of the bombarding energy and with an angular distribution strongly concentrated in the direction of

the incident neutrons, would result from n-p collisions with charge exchange. The purpose of the experiments to be described was an investigation of the distribution in angle and energy of the latter proton group, resulting from bombardment of deuterium with a beam of neutrons of about 270 Mev energy. The quantity best determined was the yield of these protons at a number of angles, integrated over energy. The nearness of approach of this quantity to the differential n-p scattering yield furnishes a measure of the accuracy of the concepts stated above regarding the nature of high energy n-d collisions; the differences that appear furnish indications of the roles played by effects such as that of the exclusion principle acting on the two neutrons left behind in the collision, and that of the internal momentum distribution of the neutron. A discussion will be given in the concluding section of such of these factors as appear to influence the measured yields of protons.

## II EXPERIMENTAL PROCEDURE

The experimental procedure chosen consisted of a comparison of the yield of n-d protons in the particular energy and angular interval under consideration with the yield of protons from n-p scattering in the same interval, measurements of the two quantities being alternated during the course of each experimental run. Most of the final data is expressed in the form of ratios of these quantities, not only because of the convenient nature of such ratios, but also because of the elimination of any effect of varying efficiency of the detecting equipment. The detector efficiency at each angle and energy enters as a factor in the determination of each differential yield, and of course cancels out in the ratio.

The experiment was divided into two main sections, the first being concerned with measurements of differential yields as a function of angle and energy, and the second with measurements of yield as a function of angle, integrated over all energies above a certain cutoff value at each angle. The latter measurements contain no information that could not be derived from the former, but were resorted to through necessity; the length of time necessary to carry out a complete set of measurements, at a number of angles, of differential yields of the former sort would have been prohibitively great.

The necessity of the cutoff energy in the latter part of the experiment arises mainly through the spread in energies of the neutrons comprising the incident beam. In measuring yields from n-p scattering in a neutron beam with wide energy spread, one wishes always to count just those protons, at each angle, which are produced by neutrons lying within certain energy limits. The energy of scattered protons in n-p collisions varies as  $E_n \cos^2 \theta$ ,  $E_n$  being the incident neutron energy and  $\theta$  the angle of emergence of the proton, measured in the laboratory frame with respect to the direction of the incident neutron. Consequently, for a fixed neutron energy limit, one must vary the energy limit on scattered protons as  $\cos^2 \theta$ . The cutoff energy chosen in the present experiments was  $200 \text{ Mev} \cos^2 \theta$ , corresponding to a 200 Mev neutron cutoff, the same limit as used in the n-p scattering experiments of Kelly, Leith, Segrè, and Wiegand<sup>7</sup>. The energy limit used in measurements of n-p yields in the present experiment was chosen to agree with the n-p scattering experiments cited above, to permit direct reference to their values of the n-p differential scattering cross section.

The energy limit used in measurement of yields from n-d collisions was also chosen the same for two reasons: first, because the amount of absorber used in setting the cutoff energy affects the efficiency of the counters (nuclear collisions in the absorber material), and it is desirable to keep the counter efficiency the same for both measurements at a given angle, as explained above; and second, because fast protons from high energy n-d collisions should approach a  $\cos^2 \theta$  energy dependence, and setting a cutoff energy varying as  $200 \text{ Mev} \cos^2 \theta$  is then almost equivalent to again choosing only those protons produced by neutrons of 200 Mev energy or greater.

The integral measurements were performed with a telescope of counters, arranged so that particles emerging from a scatterer placed in the neutron beam emerging from the 184 inch synchro-cyclotron could be observed in any chosen direction. Scattered particles were required to pass through an appropriate thickness of material, usually copper, at each angle, so that only those particles having energy above a fixed lower limit could be counted. During the course of a day's run, measurements of yield at a number of different angles could be made.

Differential measurements were made with a magnetic particle spectrometer, in which particles emerging from the scatterer within a certain small solid angle in a given direction were sorted out according to their momentum.

The apparatus was not by itself able to discriminate between protons and deuterons, but theoretical and experimental evidence, which will be discussed later, indicates that practically all of the observed particles were protons, and that no more than a negligible number of

elastically scattered deuterons contributed to the observed yields.

Figure 1 shows the overall experimental arrangement as used in both sections of the experiment.

### III DETAILS OF APPARATUS

#### A. Neutron Beam

The neutron beam used was produced by placing a 2 inch thick beryllium target in the 350 Mev circulating proton beam of the cyclotron. Neutrons emerging in a direction tangent to the path of the proton beam pass through the wall of the cyclotron tank and are collimated in a series of holes through the concrete shielding around the cyclotron before emerging to strike the scatterer.

The distribution in energy of these neutrons has been measured by Kelly et al,<sup>7</sup> in connection with n-p scattering experiments and can be determined from results of the present experiment and of previous investigations by Mr. Walter Crandall and the author. Figure 2 shows a spectrum derived from data which will be presented in Section IV. It is in agreement with those given by other workers.

The beam is delivered in pulses occurring about 60 times per second, and each having a duration of about 100 microseconds. Nearly all counts registered by the counters occur during the beam pulses, with the result that real counting rates are one to two hundred times greater than apparent counting rates. The consequence of this "duty cycle factor" is the danger of accidental coincidence counts between various counters, which must be avoided by use of sufficiently low beam intensity.

### B. Monitor

In order to compare yields from various scatterers, it is necessary to have some relative measure of integrated beam intensity. The monitors used for this purpose consisted of boron-trifluoride filled proportional counters placed in holes in the concrete shielding wall. Fast neutrons entering the shielding produce slow neutrons through elastic scattering and through generation of secondary neutrons in collisions with nuclei. The slow neutrons are captured in large numbers in the counter, producing  $\alpha$  particles and resulting counts through the reaction  $B^{10}(n,\alpha)Li^7$ . Variation of the neutron beam intensity showed that the counting rate of such a monitor varied in proportion to the counting rate from a scatterer placed directly in the beam.

### C. Magnetic Spectrometer

The magnet used to obtain momentum spectra had a space between the poles measuring 2-1/2 inches by 12 inches by 30 inches. The maximum field obtainable for any considerable length of time was about 14,000 gauss. Electronic current regulation provided a field constant to about 1/2 of one percent, corresponding to an energy variation of one percent. The magnet had been used previously as a heavy particle spectrometer in the secondary particle experiments of Hadley and York<sup>3</sup>, and was at that time provided with only one series of slits, defining a single energy channel. It was felt that this arrangement was unnecessarily inefficient, and that a great improvement would be achieved through the installation of a large number of slit systems or energy channels, each to be defined by a counter tube. An entire energy spectrum could then be obtained at once, with a single field setting.

Previous use of the magnetic spectrometer involved only proportional counters, which have been used in preference to G.M. counters both because of their much shorter dead time (a counter is unable to register two ionizing events within a certain time interval of one another, corresponding to the time taken by the tube to recover its sensitive condition after a discharge) and because they offer a possibility of discriminating against acceptance of counts from relatively lightly ionizing particles. Proportional counters, on the other hand, need a much greater amount of associated electronic equipment than do G.M. counters, so that when a large number of counters are to be used expense becomes an important consideration. With this in mind, measurements of the counting rates of G.M. tubes placed in the vicinity of the neutron beam were made. They showed that even with neutron beams of maximum possible intensity, the amount of dead time due to background counts would not be prohibitively high. Accordingly the use of G.M. tubes was decided upon - in particular, the Victoreen model 1B35 tube, which combines the advantages of a short (100 microseconds) dead time and a voltage plateau very uniform from tube to tube (threshold at 800 volts, plateau flat to about 1000 volts).

In order to define, in the magnet, a path having a certain radius of curvature, one must fix three points along the proposed path. In the particle spectrometer, the first of these three points will always consist of the scatterer, and a second of one of the set of G.M. tubes. In previous experiments at lower energies the third point was defined by the gap between a pair of lead bricks. However, at the energies involved in the present experiment, it is impossible to use a physical slit of that type which does not

have very poorly defined boundaries, owing to the ability of fast protons to pass through large thicknesses of material. The result of using a gap between two bodies of absorbing material as a defining slit would be a dependence of slit width on particle energy together with a serious contribution of multiply scattered protons resulting from traversals of material near the slit edges. With this in mind the use of small, thin walled proportional counter as a slit was chosen as highly preferable. Such counters were made, cylindrical in shape, in some cases with a diameter of 1/8 inch and in others 1/2 inch. Details of construction are shown in Figure 3. The pulses originating in such a counter were fed into the G.M. tube amplifiers in such a way that no count from a G.M. tube could be registered unless a count arrived from the proportional "slit counter" within a time interval of about 2 microseconds around the start of the G.M. pulses.

Most of the pulses originating in both the G.M. and proportional tubes come from other sources than the scatterer, and these background pulses occur with sufficient frequency that the probability of a pulse from the proportional counter coming closer than 2 microseconds to a pulse of unrelated origin from one of the G.M. tubes is quite high. The resulting accidental coincidences would of course be impossible to distinguish from real coincidence counts caused by single particles passing through both counters, so that some further mechanism for distinguishing between pulses was necessary. To satisfy this need, three additional proportional counters were placed within the magnet pole gap, and connected in electronic coincidence with the first proportional counter, so that simultaneous pulses in all four proportional counters were necessary to send a "gating" pulse to the G.M.

amplifiers and permit them to register counts. Figure 4 shows the arrangement of the magnet with associated counters.

Determination of the proton energies corresponding to the various magnet channels, at given field settings, was accomplished through use of a light, flexible wire suspended in the pole gap. When a current is passed through the wire, it assumes the same shape as the trajectory of a proton, and the value of  $H_p$  along the wire is given by the ratio of wire tension to wire current.

The spectrometer provided angular resolution of about one degree.

#### D. Counter Telescope

The counter telescopes, used in measurements of integrated scattered intensities as a function of angle, consisted of a series of three or sometimes four particle counters fixed with their centers along a straight line passing through the scatterers. A particle emerging from a scatterer along this line would produce simultaneous counts ("simultaneous" here means occurring within the resolving time of electronic coincidence circuits) in all of the counters. Such counts, after amplification, were fed into an electronic coincidence circuit which recorded the occurrence of the event. The purpose of using several counters instead of just one is again, as in the case of the magnet apparatus, to eliminate a large number of unwanted counts by applying more stringent restrictions to the conditions under which a count will be accepted.

Copper absorbers were placed between the next to last and last counters in the telescope, to fix a lower limit for proton energies that would be accepted by the telescope. The thickness was adjusted at each

angle according to the table of range-energy relations of Aron, Hoffman, and Williams<sup>8</sup> so that the total amount of material between the last counter and the center of the scatterer was always equal to the range of protons of energy  $200 \text{ Mev} \cos^2 \theta$ .

The set of counter tubes forming the telescope was mounted on a movable arm, pivoted directly under the scatterer. Thus the telescope could readily be shifted from one scattering angle to another.

Part of the experimental data was obtained using proportional counters in the telescope. It was later found that advantage could be taken of the shorter coincidence resolving time and dead time of anthracene scintillation counters to permit the use of a more intense neutron beam without difficulties from accidental coincidences and loss of counter efficiency through dead time ("blocking"). Thus data could be accumulated at a somewhat faster rate, and the proportional counters were accordingly replaced by scintillation counters.

Angular resolution obtained with the counter telescope was about three degrees.

#### E. Scatterers

The scatterers used to determine yields of protons from n-p collisions consisted of blocks of carbon and of polyethylene ( $\text{CH}_2$ ) or of paraffin wax ( $\text{-CH}_2.08$ ), the yield from hydrogen being obtained by taking the carbon-hydrocarbon difference. Yields from n-d collisions were obtained through the use of water and of heavy water scatterers, a subtraction here eliminating the oxygen effect and giving the difference between yields from deuterium and hydrogen. The water and heavy water were held in thin-walled

containers, a third identical container being left empty for use as a blank.

The scatterers were made of such a size that their horizontal dimensions were always less than the 2-1/2 inch width of the neutron beam, while vertically they projected well beyond the 1-1/2 inch height of the beam. Thus the amount of a given scatterer material exposed to the neutron beam was known and readily reproducible - experimental tests involving horizontal displacements of the scatterers showed that their position was not critical, that a considerable displacement had no effect on measured intensity of scattering. The thickness of the scatterers in the direction of emerging particles was chosen for each material so that protons of a given energy suffered equal energy loss in passing through the various scatterers. Actual thicknesses will be given with data in the next section.

#### IV REDUCTION OF DATA

##### A. General Treatment of Data

The yield from each scatterer, normalized to yield per incident neutron through division by appropriate monitor values, will be denoted by symbols  $[H_2O]$ ,  $[D_2O]$ ,  $[CH_n]$ ,  $[C]$ ,  $[B]$   $[K]$  where  $[B]$  indicates background yield with no scatterer in place and  $[K]$  indicates yield with the empty can in place.

To obtain actual yield per mole from each scatterer, we must subtract the background presumably due to scattering in the air or in the empty can, and then divide by the number of moles of scatterer intercepted by the beam, thus:

$$CH_n = \frac{1}{N_{CH_n}} ([CH_n] - [B])$$

$$C = \frac{1}{N_c} ([C] - [B])$$

$$H_2O = \frac{1}{N_{H_2O}} ([H_2O] - [K])$$

$$D_2O = \frac{1}{N_{D_2O}} ([D_2O] - [K])$$

The following subtractions then give yield per mole due to  $H_2$ :

$$\begin{aligned} H_2 &= \frac{2}{n} (CH_n - C) \\ &= \frac{2}{n} \left( \frac{1}{N_{CH_n}} [CH_n] - \frac{1}{N_c} [C] - \frac{N_c - N_{CH_n}}{N_c N_{CH_n}} [B] \right) \end{aligned}$$

and the difference between  $H_2$  and  $D_2$  yield:

$$H_2 - D_2 = \frac{1}{N_{H_2O}} [H_2O] - \frac{1}{N_{D_2O}} [D_2O] - \frac{N_{D_2O} - N_{H_2O}}{N_{D_2O} N_{H_2O}} [K]$$

To obtain the ratio of deuterium to hydrogen yield:

$$\frac{D}{H} = 1 - \frac{H_2 - D_2}{H_2}$$

and to obtain the yield due to deuterium:

$$D_2 = H_2 - (H_2 - D_2) \quad (\text{not normalised})$$

The results of the integral measurements made with the counter telescope are always to be expressed in terms of the quantities  $\frac{D}{H}$ , which may be thought of as the ratio of the fast proton component of the n-d cross section to the differential n-p scattering cross section:

$$\frac{d\sigma_{n-d}(p)}{d\Omega} \bigg/ \frac{d\sigma_{n-p}}{d\Omega}$$

The results of measurements made with the magnet are probably most significant when expressed in terms of the relative quantities  $D_2$  or  $H_2$ , so that the actual shapes of spectra are shown. The yield measured

for each energy channel must, of course, be divided by the counting efficiency of that channel, in order that the values for various energies bear the proper relative magnitudes.

#### B. Energy Intervals Accepted by Magnet Channels

Each channel of the magnet accepted protons within a certain energy interval, the efficiency within this interval being a bell-shaped curve equal to the triple cross convolution integral (fold) combining the energy uncertainties introduced by each of the three slits. Additional spread in the acceptance interval of each channel was caused by the thickness of the scatterer, and an additional function describing this was combined with the acceptance function of the magnet channels proper. The energies at half height of the resulting efficiency curve were taken as the upper and lower limits of the energy interval to which the data from each channel refers, and will be indicated in presentation of the data. Energy intervals corresponding to the scatterer thickness (about one inch for carbon) were obtained from the range-energy curves of Aron et al.<sup>8</sup>

The separate channels toward the low energy side of the magnet accepted rather narrow energy intervals, and gathered very few counts. It was thought best to combine data in several groups of channels, thus gaining in statistical accuracy. Data from each group, being actually the sum of counts from several adjacent G.M. tubes, was of course treated in the same way as data from the channels composed of single G.M. tubes, with appropriate combined energy widths and efficiencies being used.

#### C. Derivation of Efficiencies for Magnet Channels

The efficiencies of the various magnet channels for counting protons produced in a particular volume element of a scatterer are

proportional to the respective energy intervals of protons accepted. The effective energy interval of each channel varies with position in the scatterers of the volume element referred to, and hence must be averaged over the thickness of the scatterer in the following way to obtain the relative channel efficiency for a given scatterer: Consider the spectrometer in use, with protons of some energy distribution being produced throughout the volume of the scatterer. The number of protons ejected in the direction of the magnet, from a given scatterer element  $dt$  and lying within the energy interval bounded by  $E$  and  $E + dE$ , may be written as

$$F(E) dt dE$$

We will approximate the acceptance function of a magnet channel by saying that it accepts all protons of energies between  $E_0$  and  $E_1$  with 100 percent efficiency, and will accept no protons of energy outside this interval.

In addition, we make the well justified assumption that the range-energy relation for protons in the scatterer material can be written

$$R = CE^A$$

Here  $C$  and  $A$  are very slowly varying functions of energy, essentially constant within the energy limits of a given channel. Figure 5 is a plot of  $C$  and  $A$  for carbon, derived from the range-energy tables of Aron, Hoffman, and Williams<sup>8</sup>. The values of  $C$  and  $A$  plotted there were chosen to give correct values of  $R$  and  $\frac{dR}{dE}$  at each energy.

The thickness of the scatterer in the direction of the emerging protons to be counted is denoted by  $T$ , and the thickness of material traversed by protons in leaving the scatterer will be given by  $t$ . Reference may be made to the schematic diagram of Figure 6.

Consider a proton of energy  $E$  and range  $R$  as it leaves the scatterer and enters the magnet. This particle will be accepted by a given channel if

$$E_0 \leq E \leq E_1$$

When the proton originated within the scatterer element  $dt$ , its range must have been

$$R' = R + t$$

The relation between original energy  $E'$  and final energy  $E$  is then given by

$$CE'^A = CE^A + t$$

or

$$E' = (E^A + \frac{t}{c})^{\frac{1}{A}}$$

Now the number of protons originating in the element  $dt$  with energies between  $E'$  and  $E' + dE'$  is given by

$$F(E') d(E') dt$$

and the total number of protons counted by the magnet channel will be

$$N = \int_{t=0}^T dt \int_{E'=E_0'}^{E_1'} dE' F(E')$$

Let us assume that the variation of  $F(E')$  within the energy interval defined by the width of the magnet channel and the thickness of the scatterer is small and take  $F(E')$  outside the integral, replacing it by its average value  $\bar{F}$

Then

$$N = \bar{F} \int_{t=0}^T dt \int_{E'=E_0'}^{E_1'} dE'$$

$$= \bar{F} \int_{t=0}^T [(E_1^A + \frac{t}{c})^{\frac{1}{A}} - (E_0^A + \frac{t}{c})^{\frac{1}{A}}] dt$$

$$\begin{aligned}
 &= \bar{F}C \int_{t=0}^T (E_1^A + \frac{t}{c})^{\frac{1}{A}} d(E_1^A + \frac{t}{c}) \\
 &\quad - \bar{F}C \int_{t=0}^T (E_0^A + \frac{t}{c})^{\frac{1}{A}} d(E_0^A + \frac{t}{c}) \\
 &= \bar{F}C \frac{A}{1+A} \left[ (E_1^A + \frac{T}{c})^{\frac{1+A}{A}} - E_1^{1+A} - (E_0^A + \frac{T}{c})^{\frac{1+A}{A}} + E_0^{1+A} \right] \\
 &= \bar{F} \frac{A}{1+A} \left[ (CE_1^A + T) (E_1^A + \frac{T}{c})^{\frac{1}{A}} - CE_1^A E_1 \right. \\
 &\quad \left. - (CE_0^A + T) (E_0^A + \frac{T}{c})^{\frac{1}{A}} + CE_0^A E_0 \right]
 \end{aligned}$$

or making use of doubly primed quantities to indicate values at the rear of the scatterer,

$$\begin{aligned}
 R'' &= R'(T) = R+T = CE_1^A + T \\
 E'' &= E'(T) = (E_1^A + \frac{T}{c})^{\frac{1}{A}} \\
 N &= \bar{F} \frac{A}{1+A} \left[ R_1'' E_1'' - R_1 E_1 - R_0'' E_0'' + R_0 E_0 \right]
 \end{aligned}$$

Thus

$$\frac{A}{1+A} \left[ R_1'' E_1'' - R_1 E_1 - R_0'' E_0'' + R_0 E_0 \right]$$

represents the efficiency of a given channel and must be divided into the number of counts obtained to give the relative magnitude of the energy spectrum at the corresponding energy. Smoothed values of  $E_0$  and  $E_1$  for each channel were obtained from flexible wire calibration of the magnet, and values of  $E_0''$ ,  $E_1''$ ,  $R_0$ ,  $R_1$ ,  $R_0''$ , and  $R_1''$  obtained from the range-energy tables of Aron et al. Values of  $A$  used were the average value for each channel obtained from Figure 5. Values of  $R$  and  $A$  corresponding to each  $E$  were those for carbon, but since the thickness of all scatterers was adjusted to give the same stopping power, the values of efficiency derived for carbon also applied to the other scatterers.

D. Data Obtained with Magnet

Data obtained from magnet runs at scattering angles of  $4^\circ$  and  $22.5^\circ$  is presented in Tables I and II and in Figures 7 and 8, which show spectral distributions of yields from hydrogen and from deuterium. The vertical scale of each figure is completely arbitrary, and the scale of Figure 7 bears no particular relation to that of Figure 8. The relative heights of the deuterium and hydrogen spectra in each figure do represent actual relative yields, however. The statistical standard deviation and energy interval pertaining to each point is indicated in the tables.

Figure 9 shows spectra obtained in two different ways from  $D_2O$  at an angle of  $22.5^\circ$ . The upper set of points represents a spectrum taken in the normal way, while the lower set represents data taken with a carbon absorber of thickness  $24 \text{ g.cm}^{-2}$  placed between the scatterer and magnet. The latter points have been corrected for proton energy loss in the absorber, which amounts to 100 Mev for a 250 Mev proton incident at the absorber. The significance of this figure will be discussed in the next section.

Since the scattered particles from n-p collisions have energy uniquely determined by the energies of the incident neutrons, it is possible to determine the energy spectrum of a neutron source through a measurement of the energy spectrum from n-p scattering at a given angle. In order to carry out such a determination, one must have some knowledge of the form of the differential n-p scattering cross section as a function of energy at the particular scattering angle used. Figure 10 shows a curve representing this cross section for  $8^\circ$  and  $45^\circ$  scattering angles

in the center of mass system, as a function of energy. Angles of  $8^\circ$  and  $45^\circ$  in the center of mass system correspond, non-relativistically, to n-p scattering angles of  $4^\circ$  and  $22.5^\circ$  in the laboratory system. No relativistic angular correction was made in evaluating the cross sections. Figure 10 was obtained by drawing smooth curves through experimental values of the n-p cross section as obtained by various groups<sup>9</sup>.

Figure 2 shows energy spectra obtained from the  $4^\circ$  and  $22.5^\circ$  data through division by cross section values obtained from Figure 10 and application of the following additional factors, necessitated by the relativistic energies involved: the cross sections given in Figure 10 refer to unit solid angle in the center of mass system, whereas the solid angle referred to in the course of the experiment was constant in the laboratory system. Consequently the variation of center of mass solid angle corresponding to a fixed laboratory solid angle must be determined through the relation

$$\frac{d\Omega_{cm}}{d\Omega_{lab}} = \frac{2(1+\gamma) \cos \theta}{(\cos^2 \theta + \frac{1+\gamma}{2} \sin^2 \theta)^2}$$

Where

$\theta$  = laboratory scattering angle

$\gamma = 1 + \frac{\text{neutron energy}}{Mc^2}$  refers to the incident neutron

The second correction factor to be applied arises through the non-linear relation between neutron and scattered proton energies, causing a variation in neutron energy interval corresponding to unit proton energy interval.

$$T_p = \frac{T_n \cos^2 \theta}{1 + \frac{T_n}{2Mc^2} \sin^2 \theta}$$

$$\frac{dT_p}{dT_n} = \frac{\cos^2 \theta}{\left(1 + \frac{T_n}{2Mc^2} \sin^2 \theta\right)^2} = \frac{\cos^2 \theta}{\left(\cos^2 \theta + \frac{1+\gamma}{2} \sin^2 \theta\right)^2}$$

$T_n$  and  $T_p$  being the kinetic energies of the incident neutron and scattered proton.

The distribution of scattered protons is then related to the distribution of incident neutrons as:

$$\frac{dN_p}{dT_p d\Omega_{lab}} \propto \frac{dN_n}{dT_n} \cdot \frac{dT_n}{dT_p} \cdot \frac{d\sigma}{d\Omega_{cm}} \cdot \frac{d\Omega_{cm}}{d\Omega_{lab}}$$

or

$$\begin{aligned} \frac{dN_n}{dT_n} &\propto \frac{dN_p}{dT_p d\Omega_{lab}} \cdot \frac{dT_p}{dT_n} \cdot \frac{d\Omega_{lab}}{d\Omega_{cm}} \\ &\frac{d}{d\Omega_{cm}} \\ &= \frac{dN_p}{dT_p d\Omega_{lab}} \cdot \frac{\cos \theta}{2(1+\gamma)} \\ &\frac{d\sigma}{d\Omega_{cm}} \end{aligned}$$

#### E. Considerations on Presence of Scattered Deuterons

Up to this point the scattered particles have been referred to as protons. There was, however, no provision made for excluding other particles, and it would seem important to try to form an estimate of the number of deuterons that might be present among particles emerging from

n-d collisions.

First let us refer to the spectra presented in Figures 7, 8, and 9. The horizontal scales are labeled in terms of proton energies for convenience, but it must be remembered that the actual sorting is according to momentum rather than energy, as each channel represents a certain fixed value of  $H\rho$ , or momentum, for particles entering it. In the non-relativistic limit, which will be a sufficiently close approximation for the time being, protons of a given energy  $E$  will have the same momentum as deuterons of energy  $\frac{E}{2}$ . Consequently if the energy scale of the figures is divided by a factor of 2, an energy scale appropriate to deuterons will result. It is shown in Figures 7 and 8 that essentially no particles were counted with momenta corresponding to protons of energy greater than about  $350 \text{ Mev} \cos^2 \theta$ , or to deuterons of energy greater than about  $175 \text{ Mev} \cos^2 \theta$ .

The relation between incident neutron energy and elastically scattered deuteron energy is given by

$$E_d = \frac{8}{9} E_n \cos^2 \theta$$

setting an upper limit of  $\frac{9}{8} \times 175 \approx 200 \text{ Mev}$  on the energy of neutrons producing an appreciable number of deuterons through n-d scattering at angles of  $4^\circ$  and  $22.5^\circ$ . More evidence on this point can be adduced from the data presented in Figure 9. If the curve for no absorber represented only protons, one would expect its form to be preserved when the carbon absorber was used, as correction for proton energy loss in the carbon was made. No deuterons of energy less than  $240 \text{ Mev}$  can penetrate a carbon thickness of  $24 \text{ g.cm}^{-2}$ , however, so that any deuterons contributing to the spectrum obtained from  $D_2O$  without absorber should not be present

in the spectrum taken with absorber. It is seen that the two curves lie roughly parallel at proton energies greater than 225 Mev, but that a sharp break in the lower curve occurs at that point. It is felt that this break, at a deuteron energy of  $\frac{225}{2} = 113$  Mev, marks the upper limit of the spectrum of deuterons present: the corresponding neutron energy is

$$E_n = \frac{9 \times 113}{8 \cos^2 22.5^\circ} \approx 150 \text{ Mev}$$

The almost constant difference between the two curves at energies above the break is felt to represent attenuation in the carbon absorber due to nuclear scattering and inelastic processes. The attenuation factor is about  $1.6 \pm 0.3$ , which would correspond to a cross section of  $0.33 \pm 0.13$  barns per carbon nucleus for removal of scattered protons. This value is certainly within reason.

Neutrons of energy 150 Mev and lower seem to produce deuterons at  $22.5^\circ$  from heavy water; we have no information specifically as to whether the source is in the oxygen or in the deuterium. Thus the figure of 150 Mev represents only an upper limit for production in deuterium. It may be that no appreciable number of deuterons is scattered at  $22.5^\circ$  in n-d collisions by neutrons down to a considerably lower energy.

Theoretical analysis of n-d elastic scattering<sup>10,11</sup> predicts a weak maximum for deuterons projected forward (pick-up process), and a gradual decrease of cross section with deuteron angle out to well past  $60^\circ$ . This general form is characteristic, regardless of the particular interaction potential used. Consequently the upper limit of 200 Mev for neutrons producing an appreciable number of scattered deuterons at

$4^\circ$  and  $22.5^\circ$  should hold good for all angles examined in this experiment, the maximum angle at which data was taken being  $58^\circ$ . This fact will be of interest in the next section.

#### F. Data Obtained with Counter Telescope

Data obtained with the counter telescope was treated in the manner outlined in Section IV-A to give values of  $\frac{D}{H}$ .

Two separate sets of scatterers were used, one set fairly thin to provide low energy loss by scattered particles in traversing the scatterers, and another set thicker to provide a large quantity of scattering material. The former were used at wide angles, where scattered energies are low, and the latter at small angles, where scattered energies are high and energy loss in the scatterers is of relatively little importance. Particles originating at various depths in the scatterers of course traversed different amounts of material on their way out; the  $200 \cos^2 \theta$  Mev cutoff energy applied only to particles originating in the central plane of the scatterer. As a result the real cutoff took the form of a linear variation in efficiency from 0 to 1 over an energy interval, determined by the scatterer thickness, whose center lay at  $200 \cos^2 \theta$  Mev. Values of lower and upper limits of the cutoff energy interval are tabulated in Table III for both sets of scatterers.

Table III also sets forth values of  $\frac{D}{H}$  obtained with each combination of counter type and scatterer size used, together with average values at each angle, which are also shown graphically in Figure 11. Agreement between various sets of data is shown to be good.

Errors tabulated here, as well as with the magnet data, are standard deviations derived from numbers of counts obtained. It is felt that these quantities give a good indication of degree of accuracy of the data, as they are considerably larger than estimated errors likely to have been introduced from other sources.

The absorbers used to provide a proton energy cutoff of  $200 \cos^2 \theta$  Mev also provided a lower energy limit for deuterons accepted, which corresponded at each angle to deuterons scattered by neutrons of energy 300 Mev. Since evidence presented in the previous section indicates an upper limit of 200 Mev on neutrons producing a countable number of deuterons at any angle, it is felt safe to assume that the data obtained with the counter telescope refers to scattered protons only.

The integrated  $\frac{D}{H}$  value obtained at  $22.5^\circ$  is about 0.7. Comparison with the spectra plotted in Figure 8 shows that in order to secure agreement, one must assume that part of the  $D_2$  curve results from scattered deuterons. According to this view, and as suggested by the spectra of Figure 9, one would lower the portion of the  $D_2$  curve lying below 225 Mev by an amount, increasing with decreasing energy. The result of such an operation, giving a curve purporting to represent protons alone, might well bring the shape of the  $D_2$  spectrum into close agreement with the shape of the  $H_2$  spectrum. Similar considerations apply to the spectra of Figure 7.

## V INTERPRETATION OF RESULTS

The experimental results may be described in terms of two main features: first, that the energy spectrum of the fast protons produced at small angles in n-d collisions is a fairly close reproduction, in form,

of the energy spectrum of the incident neutrons; and second, that the yield of all protons of energy greater than  $200 \cos^2 \theta$  Mev, from n-d collisions, bears at each scattering angle the ratio of about 0.7 to the yield of protons, greater than the same cutoff energy, from n-p collisions.

Owing to the wide distribution of incident neutron energies, the first of these features serves merely as a somewhat qualitative demonstration of the similarity of one component of high energy n-d scattering to the product of n-p scattering. If a more nearly monochromatic neutron beam could be obtained, it would seem well worth while to measure spectra from n-d scattering at wide angles, in order to get information on the effects of the momentum distribution of the deuteron and of the interaction between the two neutrons that are left when a proton is expelled from an n-d collision. The breadth of the present neutron spectrum effectively washes out the detailed features of the expelled proton spectrum, and makes the derivation of any information on the above effects quite un dependable. For this reason, and also because of the small number of protons produced at wide angles and consequent difficulty in accumulating good statistics, it was not thought worth while to attempt further spectral measurements.

The most interesting feature of the data seems to lie in the distribution in angle of the  $\frac{D}{H}$  values obtained with the counter telescope. If the proton bound in a deuteron behaved exactly as a free proton in scattering neutrons, one would expect  $\frac{D}{H}$  to have the value 1 at all angles. It will be of interest to examine the various perturbing factors which may be the cause of the low value obtained for  $\frac{D}{H}$ .

One of the most evident of these factors is the necessity for

satisfaction of the Pauli exclusion principle, which should affect the yield of protons in the forward direction. When a fast proton emerges from an n-d collision in a direction close to that of the incident neutron, the two residual neutrons must be in a state of low relative momentum. There is a high probability in such a case for the two neutrons to be left in an S-state of angular momentum, which will only be possible in the case of anti-parallel spins. The consequence is a depression of proton yields at small angles. A different effect must be found which will tend to lower proton yields at wide angles.

Some attention has been given to the possible effect of the motion of the proton within the deuteron upon its average cross section. Approximate calculations indicate that such an effect will be appreciable for wide angles, and will result in a lowering of differential cross section of the right order of magnitude to account for the measured values. The effect of the momentum distribution of the deuteron upon the spectrum of ejected protons is a broadening which causes some protons which would otherwise be counted to fall in energy below the cutoff. Since the incident neutron spectrum was already quite broad, this effect is thought to be of slight importance.

An additional consideration, promising to be of significance, is the following. In order to change a system composed of a neutron and a deuteron into one composed of a proton and a dineutron, one must supply sufficient energy to provide for the difference in average potential energy between the deuteron and the dineutron. This effect may be quite large; Chew<sup>12</sup> has suggested that it could account for as much as a 13 Mev downward shift, at all angles, of the scattered proton energies. Aside from

this effect, one would expect the energy spectrum of the protons to shrink in proportion to  $\cos^2 \theta$ , as will the cutoff energy. The effect of a constant 13 Mev shift in moving proton energies below the cutoff point thus increases in importance with increasing proton angle, and might well account for the observed low yields at wide angles.

## VI ACKNOWLEDGEMENTS

The author wishes to express his appreciation to the many people who have been of great assistance in the completion of the experiment, and especially to the following: Mr. John Gladis and Mr. Wilmot Hess, for their invaluable collaboration throughout all phases of the experiment; Dr. B. J. Moyer, whose encouragement and suggestions have been of the greatest aid; Dr. G. F. Chew, who suggested the experiment and has offered valuable suggestions toward its interpretation; Mr. Walter Crandall, who worked with the author during various preliminary investigations; Dr. Robert Jastrow and Dr. Peter Wolff, who have furnished helpful discussions regarding interpretation of the experiment; Mr. Boris Ragent, who collaborated in the planning of the spectrometer; Dr. Robert Richardson and Mr. William Ball, who assisted greatly through the loan of scintillation counting equipment; Mr. Hugh Farnsworth and the Electronics Group under his direction, who designed and maintained the electronics equipment used; and to the Crew of 184" cyclotron for their consistent cooperation.

TABLE I

SPECTRA FROM HYDROGEN AND DEUTERIUM AT 4°

Channel	Energy Limits (Mev)	H	D
1	354-418	0.06 ± 0.3	0.4 ± 0.4
2	318-375	2.0 ± 0.6	1.8 ± 1.1
3	285-336	8.4 ± 0.8	4.9 ± 1.5
4	259-300	13.0 ± 1.1	9.8 ± 2.1
5	234-272	11.5 ± 1.3	9.4 ± 2.3
6	214-247	9.9 ± 1.4	5.7 ± 2.5
7	167-225	4.0 ± 0.8	2.9 ± 1.5
8	72-176	6.8 ± 0.9	6.0 ± 1.6

TABLE II

SPECTRA FROM HYDROGEN AND DEUTERIUM AT 22.5°

Channel	Energy Limits (MeV)	H	D
1	308-365	0.3 ± 0.2	0.4 ± 0.2
2	279-372	1.0 ± 0.4	0.7 ± 0.5
3	249-292	5.1 ± 0.5	5.1 ± 0.7
4	226-263	12.3 ± 0.8	9.8 ± 1.2
5	206-239	13.0 ± 1.0	10.9 ± 1.4
6	187-216	10.5 ± 1.1	11.0 ± 1.5
7	144-197	8.1 ± 0.7	8.2 ± 1.0
8	60-154	6.7 ± 0.7	6.4 ± 1.0

TABLE III

## DATA FROM COUNTER TELESCOPE RUNS

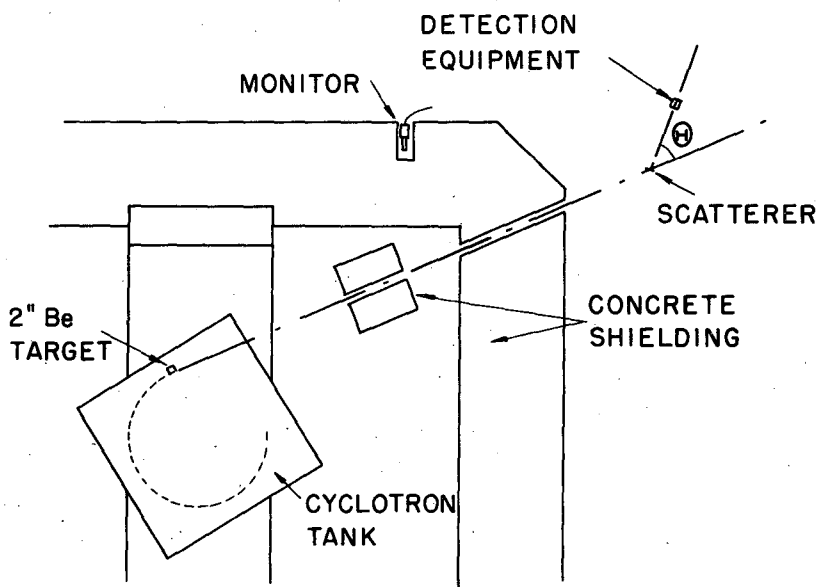
Scatterers A: 2.26 g.cm<sup>-2</sup> C equivalent  
 Scatterers B: 4.02 g.cm<sup>-2</sup> C equivalent

## Data from Various Runs

θ	Cutoff Energy, Mev		Proportional Counters	Scintillation Counters			Average
	A	B	B	A	A	B	
4°	195-205	192-209		0.774 ± 0.046		0.704 ± 0.024	0.719 ± 0.021
9°	195-205	191-209	0.670 ± 0.058	0.701 ± 0.066			0.682 ± 0.044
15°	195-205	190-209	0.708 ± 0.063	0.800 ± 0.065			0.752 ± 0.045
22.5°	194-206	189-210	0.697 ± 0.069	0.750 ± 0.086			0.715 ± 0.052
30°	193-207	187-213	0.755 ± 0.108		0.828 ± 0.091	0.926 ± 0.126	0.827 ± 0.061
35°	191-209			0.806 ± 0.113			0.806 ± 0.113
45°	185-215	173-227	0.772 ± 0.128		0.465 ± 0.150		0.643 ± 0.097
55°	169-232			0.513 ± 0.219	0.627 ± 0.142		0.593 ± 0.120
58°	158-243				0.705 ± 0.100		0.705 ± 0.100

VII REFERENCES

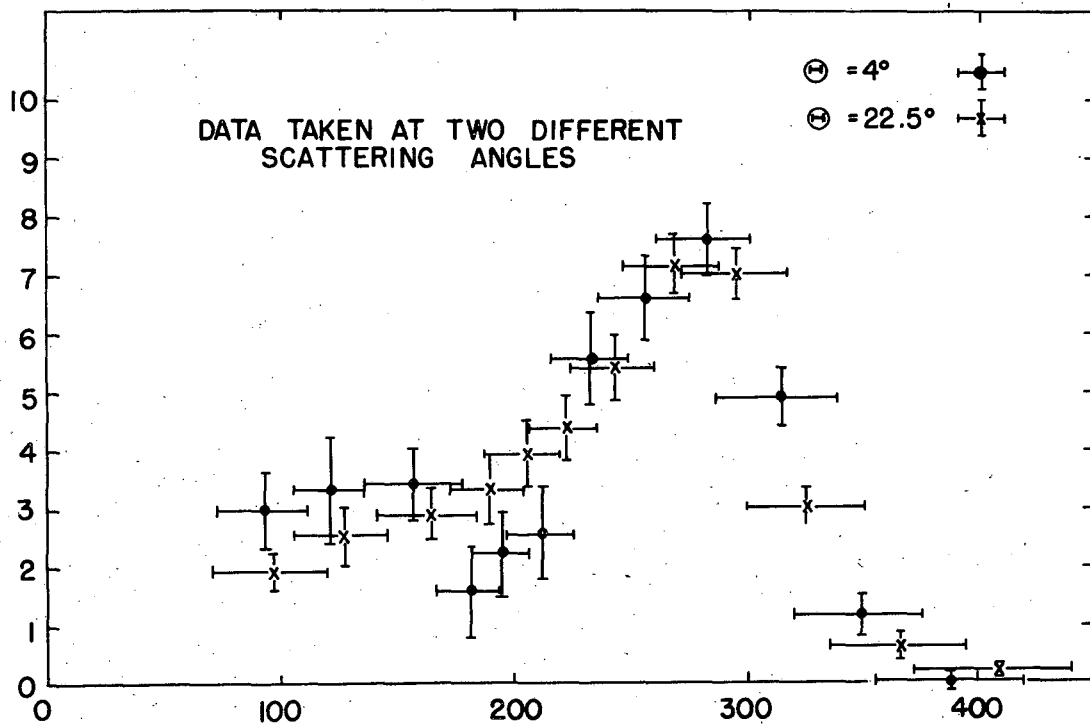
1. J. B. Gladis, J. Hadley, and B. J. Moyer, Phys. Rev. 81, 649 (A) (1951).
2. G. M. Temmer, Phys. Rev. 83, 1067 (1951).
3. J. Hadley and H. F. York, Phys. Rev. 80, 345 (1950).
4. F. de Hoffmann, Phys. Rev. 78, 216 (1950).
5. G. F. Chew, Phys. Rev. 80, 196 (1950).
6. R. C. Gluckstern and H. A. Bethe, Phys. Rev. 81, 761 (1951).
7. E. Kelly, C. Leith, E. Segrè, and C. Wiegand, Phys. Rev. 79, 96 (1950).
8. W. A. Aron, B. G. Hoffman, and F. C. Williams, U. S. Atomic Energy Commission Publication, AECU-663.
9. See R. H. Hildebrand, D. A. Hicks, W. H. Harker, University of California Radiation Laboratory Publication, UCRL-1305, Kelly *et al.* (Reference 7), and E. M. Baldwin, Phys. Rev. 83, 495 (1951), for cross section values and further references.
10. G. F. Chew, Phys. Rev. 74, 809 (1948).
11. Ta-You Wu and J. Ashkin, Phys. Rev. 73, 986 (1948).
12. G. F. Chew (private communication).



MU 2753

Fig. 1

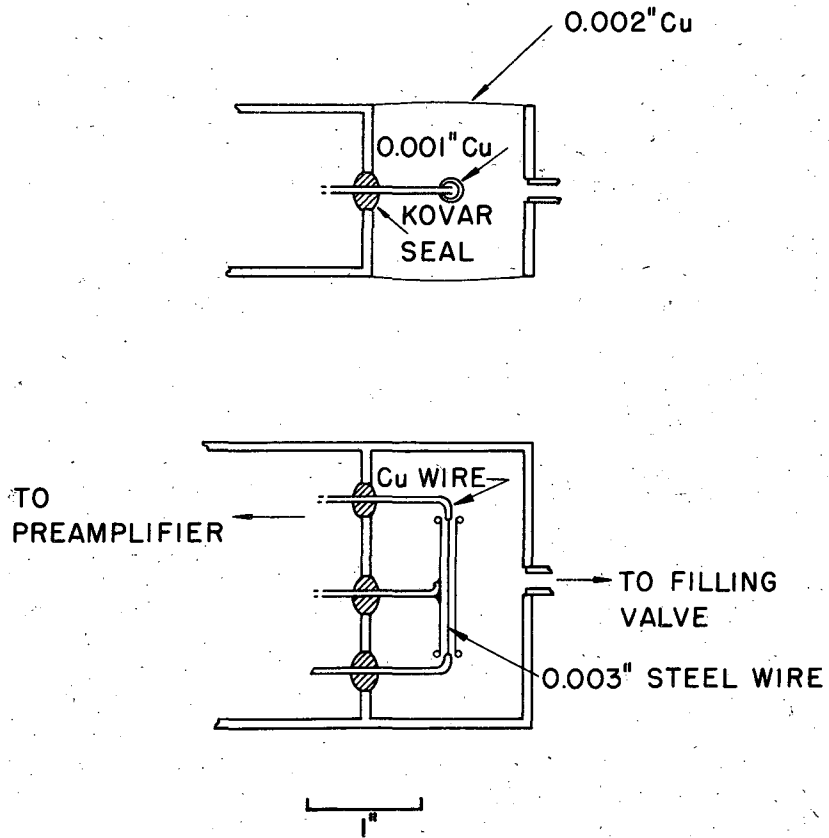
GENERAL EXPERIMENTAL ARRANGEMENT



MU 2715

Fig. 2

ENERGY DISTRIBUTION OF NEUTRON BEAM



MU 2754

Fig. 3

CONSTRUCTION OF SMALL PROPORTIONAL COUNTER.

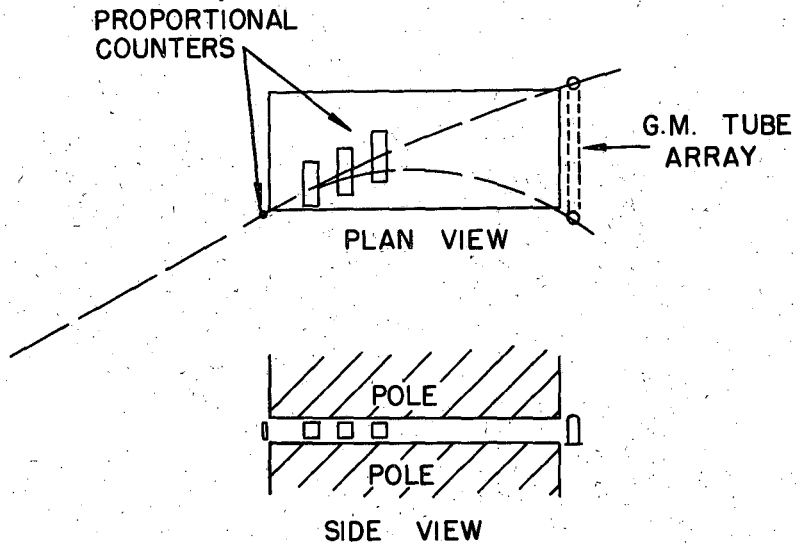


FIG. 4 MU 2716

Fig. 4

SCHEMATIC DIAGRAM OF SPECTROMETER

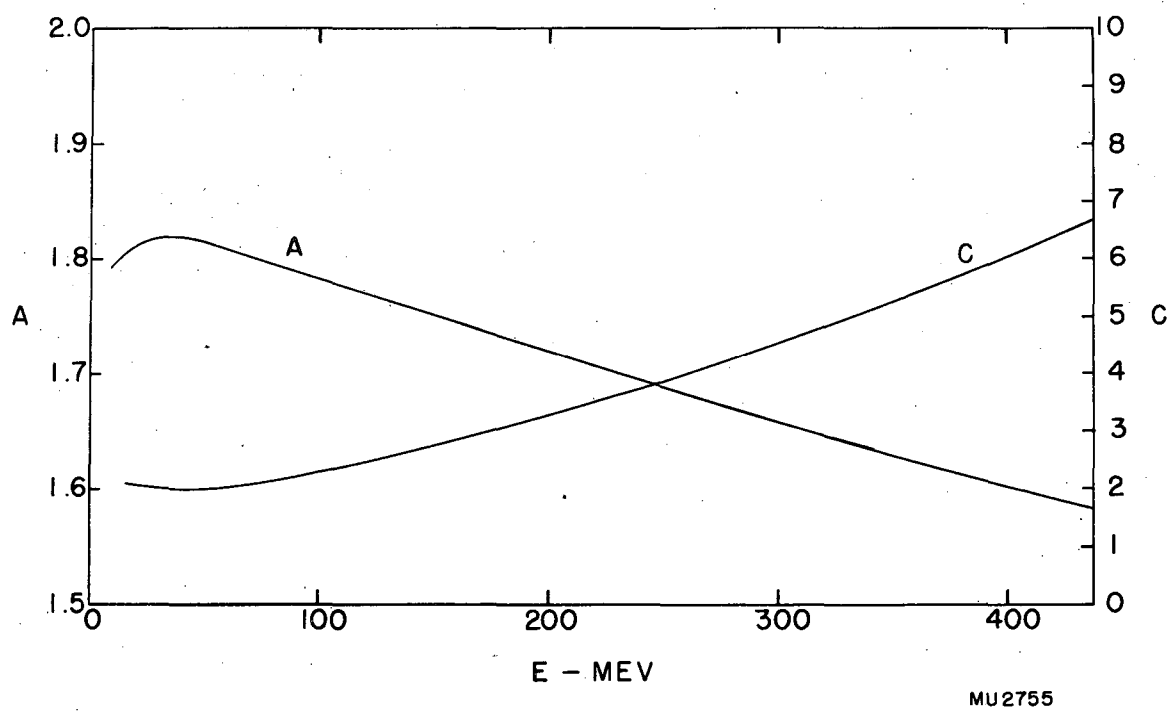


Fig. 5

C AND A AS FUNCTIONS OF ENERGY

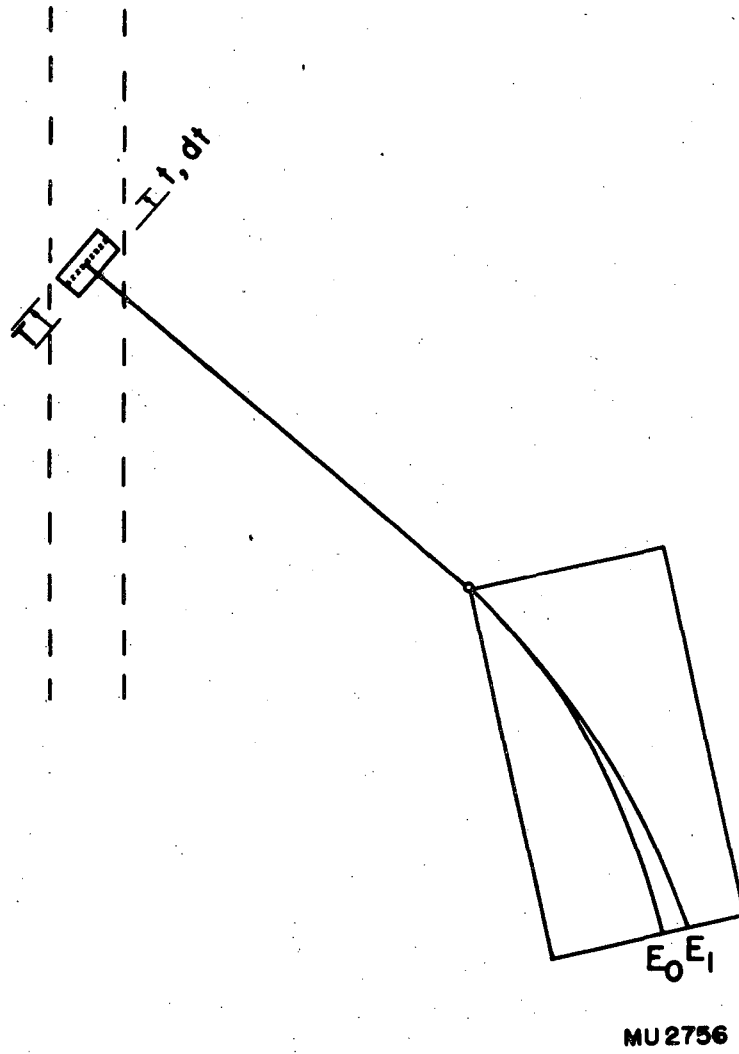


Fig. 6

DIAGRAM ILLUSTRATING CALCULATION  
OF CHANNEL EFFICIENCIES

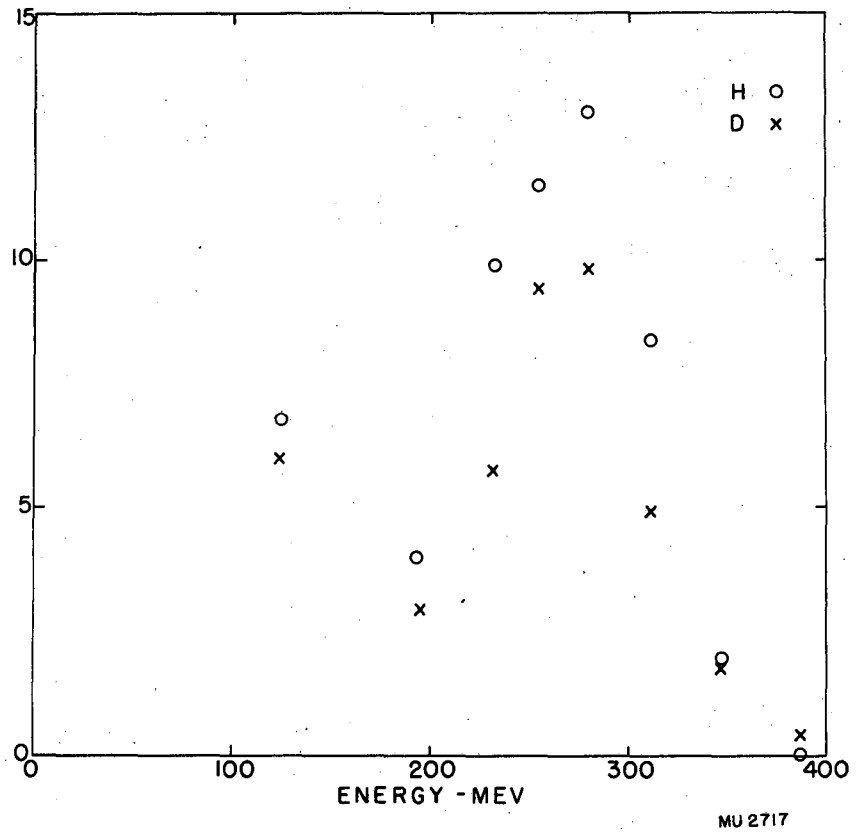


Fig. 7

H AND D SPECTRA AT 4°

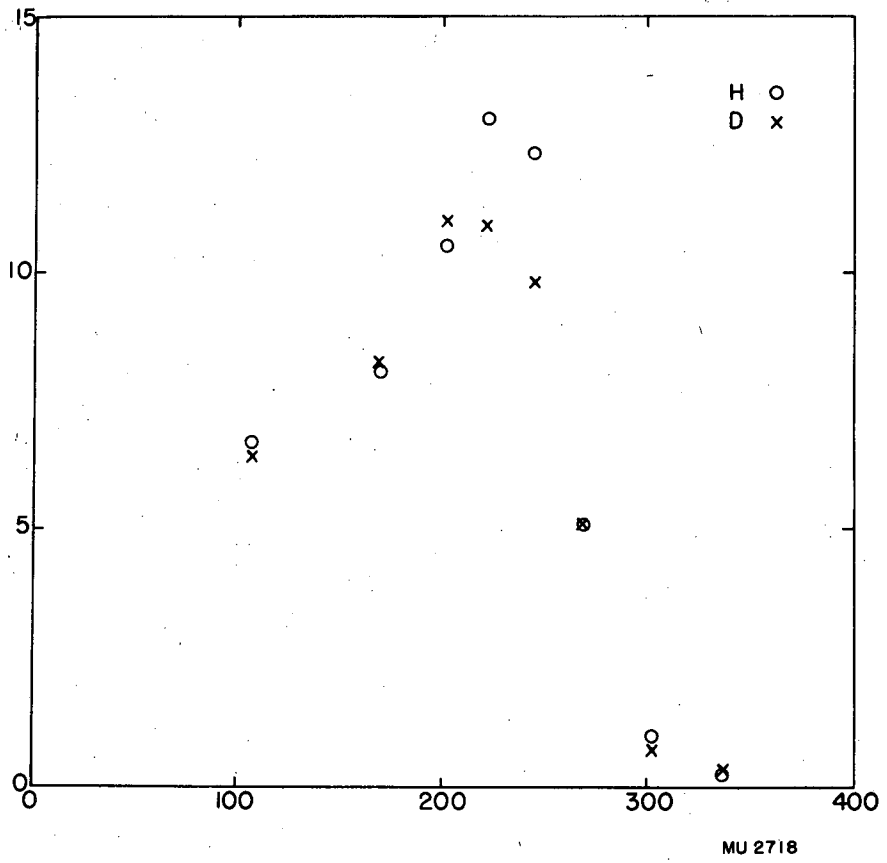


Fig. 8

H AND D SPECTRA AT 22.5°

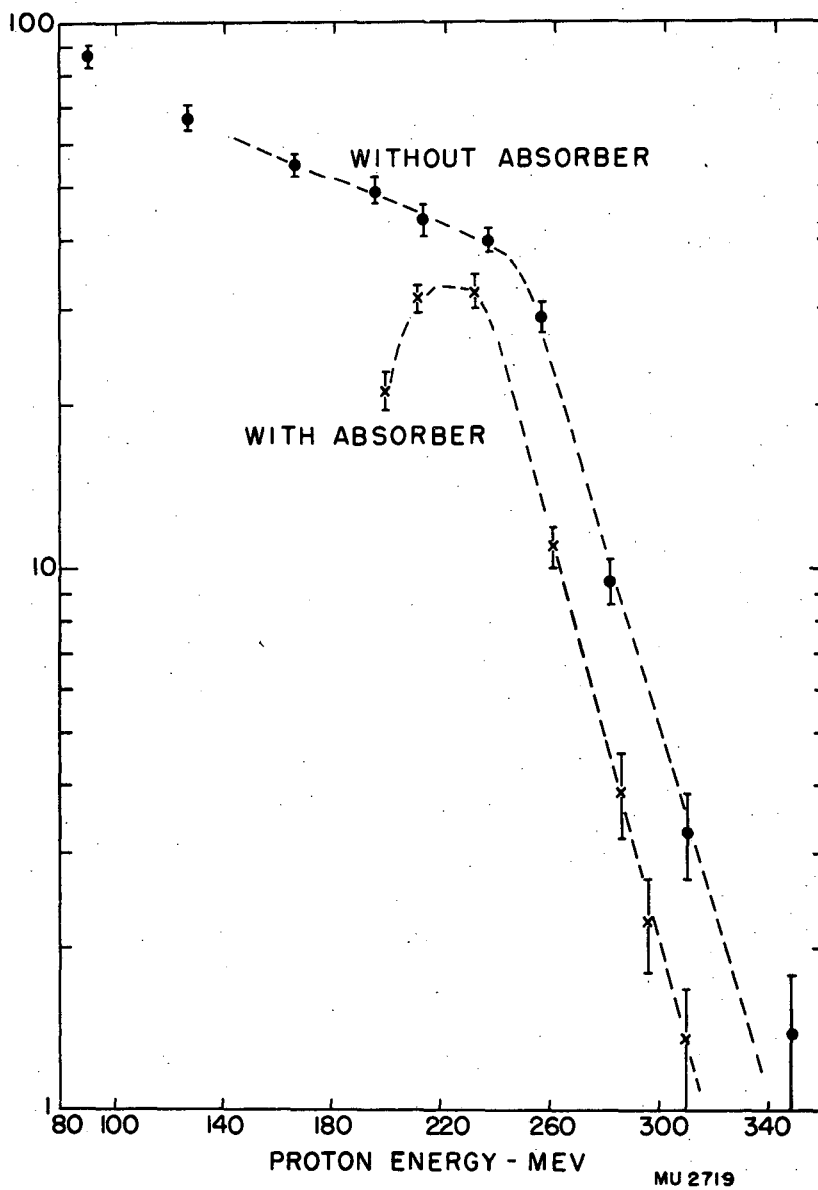
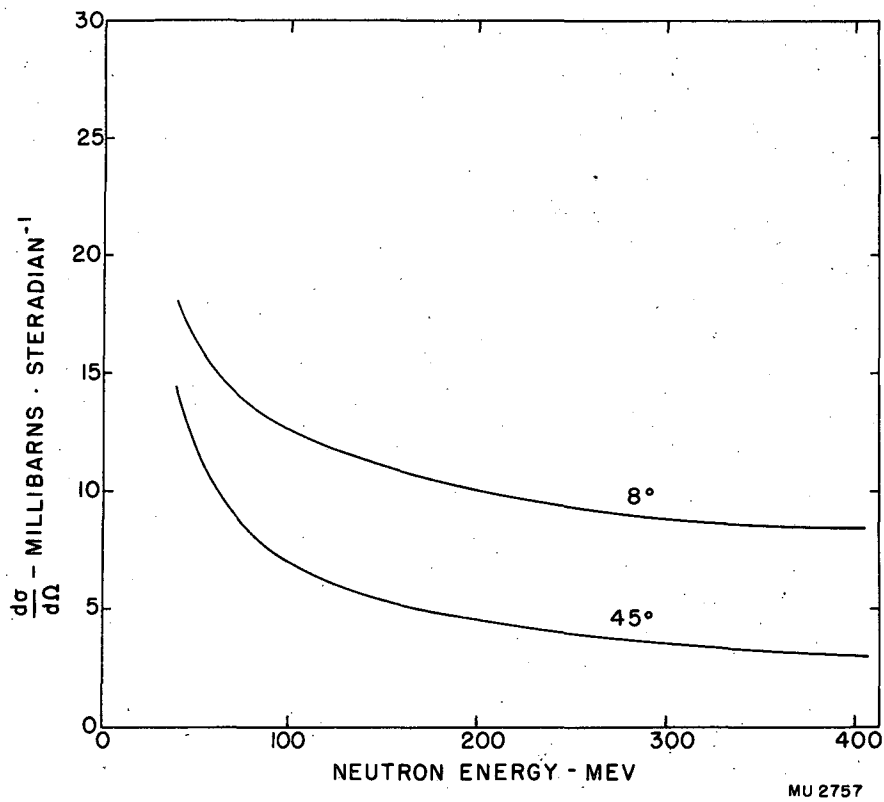


Fig. 9

EFFECT OF CARBON ABSORBER ON  
PARTICLES FROM  $D_2O$  AT  $22.5^\circ$



MU 2757

Fig. 10

VALUES OF  $\frac{d\sigma}{d\Omega \text{ cm}}$  USED IN DERIVATION  
OF NEUTRON BEAM ENERGY SPECTRUM

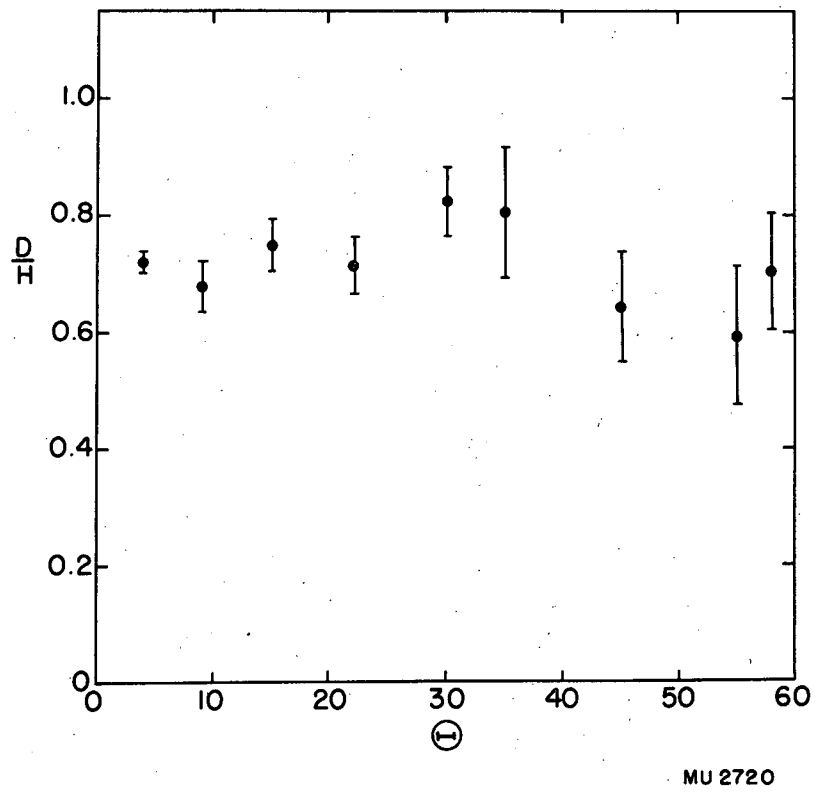


Fig. 11

$D/H$  AS A FUNCTION OF ANGLE